A new methodology for the quantitative visualization of coherent flow structures in alluvial channels using multibeam echo-sounding (MBES)

Jim Best,[1] Stephen Simmons,[2,3] Daniel Parsons,[2] Kevin Oberg,[4] Jonathan Czuba,[5] and Chris Malzone[6]

Received 23 November 2009; revised 21 January 2010; accepted 27 January 2010; published 17 March 2010.

[1] In order to investigate the interactions between turbulence and suspended sediment transport in natural aqueous environments, we ideally require a technique that allows simultaneous measurement of fluid velocity and sediment concentration for the whole flow field. Here, we report on development of a methodology using the water column acoustic backscatter signal from a multibeam echo sounder to simultaneously quantify flow velocities and sediment concentrations. The application of this new technique is illustrated with reference to flow over the leeside of an alluvial sand dune, which allows, for the first time in a field study, quantitative visualization of large-scale, whole flow field, turbulent coherent flow structures associated with the dune leeside that are responsible for suspending bed sediment. This methodology holds great potential for use in a wide range of aqueous geophysical flows. **Citation:** Best, J., S. Simmons, D. Parsons, K. Oberg, J. Czuba, and C. Malzone (2010), A new methodology for the quantitative visualization of coherent flow structures in alluvial channels using multibeam echo-sounding (MBES), *Geophys. Res. Lett.*, *37*, L06405, doi:10.1029/2009GL041852.

1. Introduction

[2] Many laboratory [e.g., *Grass*, 1970; *Kuhnle and Wren*, 2009; *Lelouvetel et al.*, 2009], field [*Parsons et al.*, 2005] and numerical [*Nakayama et al.*, 2000] studies have demonstrated the intrinsic links between bed roughness, the entrainment and transport of sediment, and the presence of coherent turbulent flow structures of differing spatio-temporal scales. Coherent flow structures appear responsible for the entrainment [*Schmeeckle and Nelson*, 2003] and transport [*Drake et al.*, 1988] of bedload and the lifting of sediment into suspension [*Lelouvetel et al.*, 2009]. Such coherent flow structures arise in both wall-bounded and free shear layers, and reveal great complexity over smooth walls (see review by *Adrian* [2007]) and both grain [*Roy et al.*, 2004] and form [*Best*, 2005; *Stoesser et al.*, 2008; *Grigoriadis et al.*, 2009] roughness. Investigating the links between the structure of turbulent flows and the transport of sediment, as bedload or suspended load, remains a key goal of many Earth surface studies, and yet detecting and quantifying the behavior of such two-phase fluids is notoriously difficult. What we ideally require are techniques, in both laboratory and natural environment, which can quantify the holistic flow field in the simultaneous measurement of velocity structure and sediment transport characteristics. In the laboratory, such experiments have begun to be conducted using phase Doppler anemometry [e.g., *Best et al.*, 1997] and two-phase particle imaging velocimetry and particle tracking [e.g., *Lelouvetel et al.*, 2009; *Muste et al.*, 2009]. In field studies, application of acoustic Doppler current profiling (ADCP) has revolutionalized the investigation of three-dimensional flow structures and begun to link these to sediment transport [see *Dinehart and Burau*, 2005; *Rennie et al.*, 2002]. However, most of these field techniques are single point, which require deployment of arrays of probes, or with an ADCP yield one instantaneous profile.

[3] Recent advances in multibeam echo-sounding (MBES) acoustics have yielded shallow-water MBES systems that can reveal unprecedented detail of the bed morphology [*Parsons et al.*, 2005; *Bartholomä et al.*, 2004] and bedform migration [*Nittrouer et al.*, 2008], whilst the backscatter signal from the bed can also be utilized to provide information on the bed roughness [*Fonseca and Mayer*, 2007]. However, MBES systems also provide acoustic returns from within the water column that can image within the flow, and this ability has recently been applied for both object detection [*Brissette et al.*, 2001] and visualization of black smokers [*Jackson et al.*, 2003]. Our recent work [*Simmons et al.*, 2010] has further demonstrated how the backscatter signal can be used to provide estimates of the sediment concentration field within the MBES swath, and yield new visualizations of the suspended sediment structure and dynamics. Here, we report on the first use of the MBES water column acoustic backscatter signal to concurrently quantify two-dimensional velocities within the multibeam swath and suspended sediment concentration. We illustrate this capability with reference to flow over the leeside of an alluvial sand dune, and demonstrate how MBES has the unique capability to quantitatively visualize the whole flow field dynamics and

[1]Departments of Geology and Geography and Ven Te Chow Hydrosystems Laboratory, University of Illinois at Urbana-Champaign, Urbana, Illinois, USA.
[2]School of Earth and Environment, University of Leeds, Leeds, UK.
[3]Now at Aquatec Group Ltd., Hartley Wintney, UK.
[4]U.S. Geological Survey, Urbana, Illinois, USA.
[5]U.S. Geological Survey, Tacoma, Washington, USA.
[6]Myriax Software Pty Ltd., San Diego, California, USA.

0094-8276/10/2009GL041852

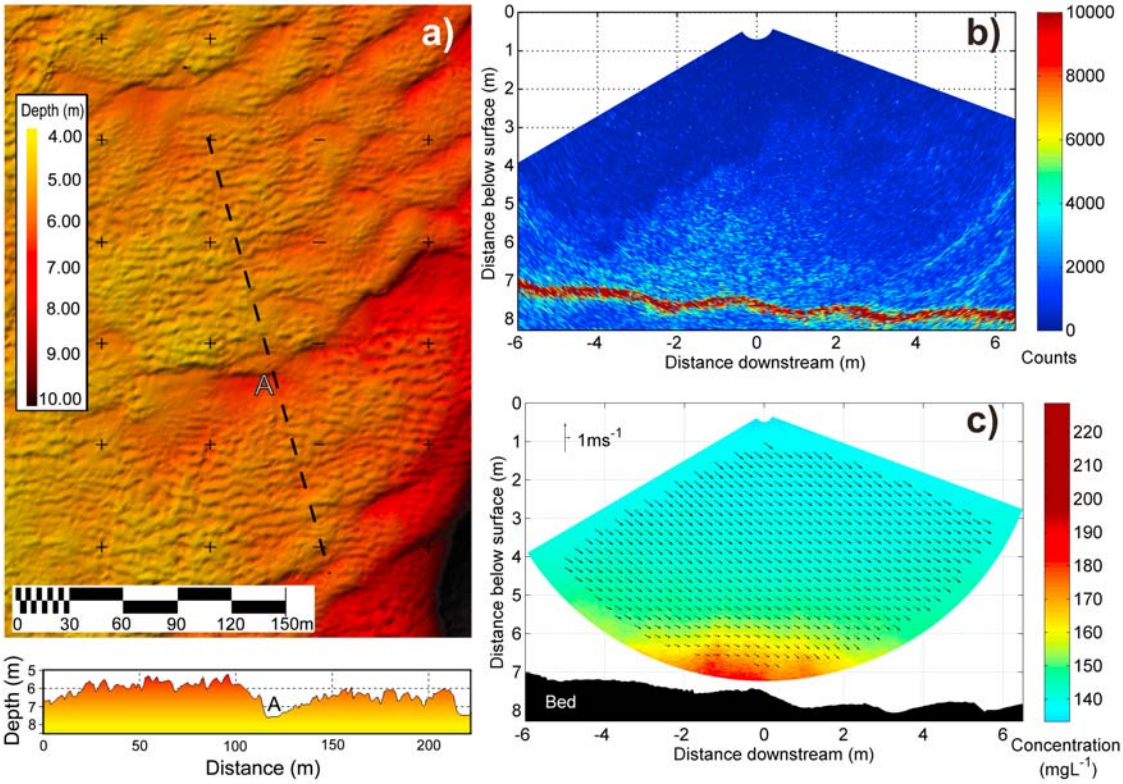

Figure 1. (a) MBES map of the bed morphology of the dune field at the measurement position, showing large dunes with superimposed smaller dunes. Flow direction top left to bottom right. The longitudinal profile shows the leeside of the dune measured herein marked "A." The UTM position of the dune was 4299381N, 750281E. Depths are the same as "distance below surface" in Figures 1b, 1c, and 2. (b) Image of the MBES swath after the acoustic return has been adjusted for acoustic propagation losses (spherical spreading and time-varying gain). Scale is in analogue-to-digital converter counts, showing the magnitude of the backscatter signal. (c) Vectors of the mean flow field after application of the velocity determination methodology. The colored background shows the mean suspended sediment concentration (for methodology see *Simmons et al.* [2010]). The vertical component of velocity used for these vectors is exaggerated by a factor of 5 to assist visualization. Flow left to right.

allow investigation of the association between turbulent coherent flow structures and sediment in transport.

2. Field Site and Equipment

[4] We report on measurements of flow and sediment transport over the leeside of a sand dune (Figure 1a) located close to the confluence of the Mississippi and Missouri Rivers, Missouri, USA during a survey on October 20th 2007. A RESON 7125 400 KHz MBES was mounted at the bow of a stationary, moored, survey vessel, with dynamic positioning being given by a Leica System 1230 real-time kinematic GPS, which provided relative horizontal positional accuracy to within 0.02 m. A Teledyne RD Instruments 1200 kHz acoustic Doppler current profiler (ADCP) was mounted from the side of the vessel, and there was thus a lateral and downstream offset of the ADCP from the MBES of 1.25 and 0.79 m respectively. The MBES formed 256 beams over a 128 degree swath, and the MBES head was mounted so that the swath was orientated parallel to flow and 0.30 m below the water surface. The swath width covered ~4 times the flow depth, which was approximately 7 m at this locality, therefore yielding an echogram "field-of-view" of ~28 m.

[5] The bed morphology was characterized by a field of sand dunes that were ~40 m in wavelength, 1.7 m high and typically had asymmetrical profiles, with steeper downstream lee slopes (~8–15°) and shallower (~2–5°) upstream stoss slopes (Figure 1a). The boat was moored over the leeside slope of one of these dunes (Figure 1a), which had a leeside slope of 9.8° and also exhibited smaller superimposed bedforms that were ~0.35 m in height (Figures 1a and 1b). At this moored location, time series of MBES and ADCP backscatter signal were collected. Due to possible acoustic interference between the MBES and ADCP, the ADCP measurements were taken immediately after completion of the MBES data collection, although during this time (~15 minutes in total) the flow was constant in velocity and discharge. The MBES and ADCP operated at data rates of 10 and 3.125 Hz respectively, with the extent of the sampling bins being 0.021 m and 0.2 m respectively for MBES and ADCP.

3. MBES Acoustic Method for the Determination of Flow Velocity

[6] The raw backscatter data from the MBES swath was collected using RESON 7k Center™ MR v3.5 software, with the full backscatter data requiring approximately 650 MB of

storage for every minute of data. Subsequent analysis has developed procedures for data processing that yield estimates of sediment concentration and flow velocity across the width of the MBES swath. Full details of the determination of sediment concentration are given by *Simmons et al.* [2010] and here we detail our new methodology for deriving flow velocity, which consisted of two stages.

3.1. Stage I: Data Processing Prior to Application of the Velocity Estimation Algorithm

[7] Firstly, the signal was examined to determine the nearest distance from the transducers to the bed and then the regions of side-lobe interference [*Hughes-Clarke*, 2006] were removed, yielding a wedge-shaped area, approximately 12m wide at the bed, where the backscatter signal was dominated by material suspended in the water-column (Figure 1b). These data were used to calculate the magnitude of the scattering volume (Sv) from the raw acoustic backscatter signal, which is defined as the acoustic backscatter strength per unit volume of ensonified water, using the sonar parameter settings and acoustic propagation losses. Full details of this methodology are given by *Simmons et al.* [2010]. Once the magnitude of the scattering volume was determined for all the data, a two-dimensional interpolation of the data was performed to convert the co-ordinates from a polar to a rectangular grid.

3.2. Stage II: Estimation of Flow Velocity

[8] Velocities within the MBES swath were determined using an approach similar to that routinely applied in particle imaging velocimetry [*Westerweel*, 1997], where the displacement of groups of particles is examined between adjacent interrogation areas over a known time interval. In our MBES application, the Sv values were utilized to provide a 'tracer' between successive MBES acoustic pings, and ten steps were used to calculate two-dimensional velocities (herein downstream and vertical) across the MBES swath:

[9] 1. A grid was created across the area of the wedge-shaped swath that corresponded to the center points of square interrogation areas (whose area herein was nominally 4 m^2). Each of these points corresponded to the location of an area that would provide a single vector estimate of velocity.

[10] 2. For each of these single points, the location of all the data within the rectangular interrogation area that was centered on this point was determined. The shape of this data area was irregular where the extent of the rectangle overlapped the edge of the swath.

[11] 3. In the next consecutive acoustic ping, all areas of data defined by the rectangles established in step 2, and within a user-specified horizontal and vertical displacement of this area in the first ping, were determined.

[12] 4. The maximum mean quadratic difference (MQD) [*Gui and Merzkirch*, 1996] was then calculated between the area defined in the first ping and all bordering squares in the second ping. Where the area in the second ping was closer to the edge of the swath, and hence smaller in size, the area within the first ping was re-adjusted to be the same dimensions.

[13] 5. The area within the second ping that possessed the highest correlation with the first ping was then determined, with the estimate being discarded if the correlation value was below a user-defined threshold (herein set as 0.25).

[14] 6. The centroid of this area was then determined, as it will differ from the center of the square where it overlaps the edge of the swath. The direction and magnitude of this vector was then determined from the position of the centroids in the first and second pings and the time between pings (herein 0.1 s).

[15] 7. Steps 2–6 were then repeated until the entire grid of interrogation areas in the first ping had been filled.

[16] 8. Once all interrogation areas had been filled using these two pings, the estimated velocity vectors were interpolated back onto a rectangular grid, again noting that the centroids of the interrogation areas will be irregular where they overlap the edge of the swath.

[17] 9. Steps 1–9 were then repeated for all successive pings in the time series.

[18] 10. Lastly, a temporal moving average, here of 9 time steps (0.9 s), was performed on consecutive estimates of velocity, yielding an average velocity field within the MBES swath (Figure 1c).

[19] This procedure yielded maps of two-dimensional velocity across the swath at the ping rate used, and these velocity vectors could be overlain on the suspended sediment concentration field to yield quantitative visualizations of the evolving flow field in the lee of the dune (Figures 1c and 2). The results from analysis of 43 water samples, used to calibrate the suspended sediment concentration, showed 85% of sediment in the water column was finer than 0.063mm in diameter (range 60–99%). It can thus be assumed that these finer particles will track the water flow and any slip between the water and sediment phases will be minimal, an assumption that is also made in estimating water velocities using an ADCP.

4. Results and Discussion

[20] The map of mean flow in the dune leeside derived from the MBES (Figure 1c) shows general downward flow towards the bed that is to be expected in this region, and it is noticeable that in this low-angle leeside there is no evidence for any time-averaged flow separation zone with upstream flow, a feature found in previous experimental studies of low-angle dunes [*Best and Kostaschuk*, 2002]. Moreover, the presence of the small superimposed bedforms on the leeslope (Figure 1a) does not appear, at this spatial resolution, to have any influence on the time-averaged flow field. Flow velocities decline towards the bed and the time-averaged sediment concentration field (Figure 1c) shows higher values, approaching 210 mgL^{-1}, near the bed, although these values decline rapidly above ~2m from the bed.

[21] Maps derived from successive pings (Figure 2; see also Animation S1 of the auxiliary material) clearly visualize distinct events of flow upwelling in this near-bed region that are associated with significantly higher sediment concentrations (250–320 mgL^{-1}) than the surrounding flow (~150 mgL^{-1}).[1] The event shown here (Figure 2) has an upstream slope angle of ~39 degrees with the highest sediment concentrations within this coherent flow structure being nearer the bed. Flow within the region of high sediment concentration is upwards and away from the bed (labeled "i"

[1] Auxiliary materials are available in the HTML. doi:10.1029/2009GL041852.

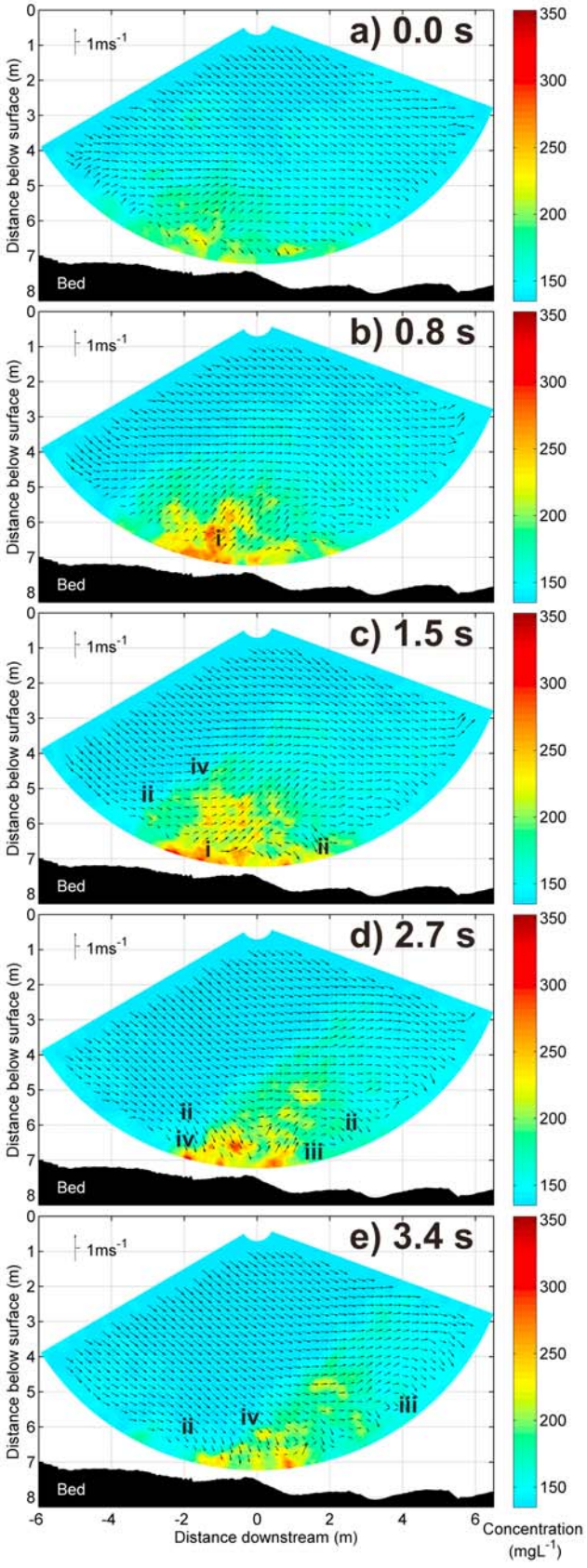

in Figures 2b and 2c), whilst flow both downstream of this region, as well as upstream on the back of the structure, is down towards the bed (labeled "ii" in Figures 2c–2e). The downstream edge of the structure also appears to have some spanwise rotation associated with it (labeled "iii" in Figures 2d and 2e), as well as some regions of irregular topology on its upstream side (see irregular boundary between green/yellow and blue colors, labeled "iv" in Figures 2c–2e), that are likely to be associated with secondary vorticity on top of this large primary coherent flow structure. These flow visualizations provide, for the first time, a quantitative whole-flow field confirmation of large-scale vorticity associated with dunes that has only been achieved in past laboratory [*Kadota and Nezu*, 1999; *Best*, 2005] and numerical studies [*Stoesser et al.*, 2008; *Grigoriadis et al.*, 2009]. Such upwellings of low momentum fluid away from the bed have been linked to Kelvin-Helmholtz instabilities formed along a shear layer in regions of flow separation or flow expansion [*McLean et al.*, 1994; *Bennett and Best*, 1995] or upstream stacked wakes [*McLean et al.*, 1996] and flow expansion in the leeside of low-angle dunes [*Best and Kostaschuk*, 2002]. Such upwellings also then demand subsequent inrushes of fluid from higher in the flow to return towards the bed, and this is clearly shown in these MBES-derived flow fields. An animation of such large-scale coherent flow structures, and their associated sediment transport field over a period of 10 seconds (Animation S1), shows a sequence of coherent flow structures that advect away from the bed, have a characteristic shape as described above with upstream sloping surfaces, and possess higher suspended sediment concentrations. The topology of these turbulent events bears similarities in their two-dimensional shape to classic large-scale turbulent boundary layer vorticity [e.g., *Adrian*, 2007]. However, it is likely that the origin of this turbulence lies in flow expansion in the dune leeside, possibly associated with a temporary shear layer [*Best and Kostaschuk*, 2002] that generates large-scale turbulence that may advect to the water surface, as seen at this survey site during these measurements (see Animation S2 of the auxiliary material).

[22] To assess the accuracy of this MBES velocity estimation, we have compared the MBES-derived mean velocities with those obtained from the ADCP. To achieve this, we used the MBES interrogation areas on either side of the nadir beam that would represent the same 2D spatial volume as the ADCP acoustic cone, using a similar length time series (herein 1 minute) to compute mean values. Comparison of the downstream and vertical velocities from the two methodologies (Figure 3) shows good agreement, with mean downstream velocities within the profile exhibiting maximum differences of 10%. Correlation between the MBES and ADCP downstream velocities yields

Figure 2. Five images of flow and suspended sediment fields across the MBES swath with time increments given on each image. These images show the downstream advection of a large-scale coherent flow structure that possesses a higher sediment concentration than the surrounding flow field. In order to assist visualization of the flow structure, the vertical component of velocity used for these vectors is exaggerated by a factor of 5 and has had the mean vertical velocity across the entire swath subtracted from each value. Flow left to right. See text for explanation.

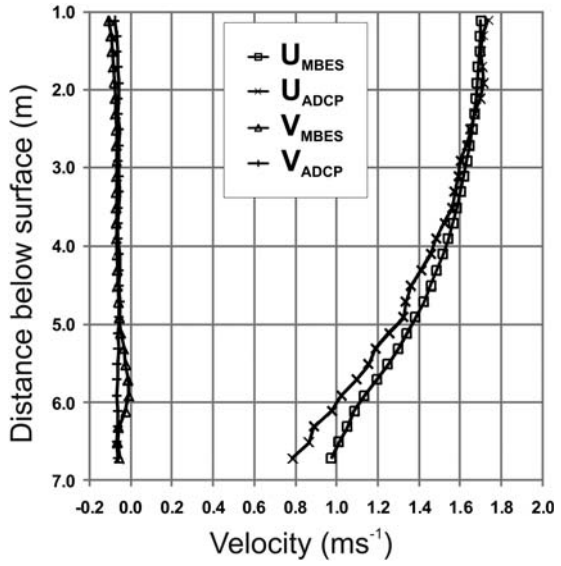

Figure 3. Comparison of mean velocity profiles for the downstream (U) and vertical (V) components of velocity between the MBES (subscript MBES) and acoustic Doppler current profiler (subscript ADCP).

an R^2 of 0.99, with the MBES and ADCP matching very well in the upper flow, but deviating towards the bed (by up to 0.14 ms^{-1}), where more spatial changes in dune-related mean flow could be expected. The vertical components of velocity are low, but similar in magnitude, although the ADCP does not appear to detect the variation that is shown by the MBES results. The correspondence between the mean MBES- and ADCP- derived velocities is thus highly satisfactory, especially considering that the MBES and ADCP samples were not coincident in either space or time.

5. Conclusions

[23] We have demonstrated herein a new quantitative methodology for using multibeam echo sounding to obtain whole flow field estimates of two-dimensional fluid velocities across the MBES swath that, together with recent developments for estimating suspended sediment concentrations [*Simmons et al*., 2010], yields the first quantitative visualizations of such flows at the field scale. We illustrate this new technique through visualization of flow in the leeside of a low-angle sand dune that is seen to generate large, macroturbulent flow structures. This at-a-point technique yields whole flow field quantification of both suspended sediment and 2D velocities that may have many other potential applications in environments where distinct differences in water column acoustic backscatter are present, such as those associated with bedforms, secondary flow circulations [*Dinehart and Burau*, 2005], and free shear layers between mixing flows [*Simmons et al.*, 2010]. The methodology we describe herein thus offers a powerful new tool in unraveling the complex links between mean flow, turbulence and sediment transport in many aqueous flows on the Earth's surface.

[24] **Acknowledgments.** This research was conducted as part of UK NERC grant NE/D014530/1 to JB and DP. We are very grateful to Kevin Johnson for his field assistance, and to the United States Geological Survey Office of Surface Water for their support. Use of trade, product, or firm names in this paper is for descriptive purposes only and does not imply endorsement by the U.S. Government.

References

Adrian, R. J. (2007), Hairpin vortex organization in wall turbulence, *Phys. Fluids*, *19*, 041301, doi:10.1063/1.2717527.

Bartholomä, A., V. B. Ernstern, B. W. Flemming, and J. Bartholdy (2004), Bedform dynamics and net sediment transport paths over a flood-ebb cycle in the Grådyb channel (Denmark), determined by high-resolution multibeam echosounding, *Dan. J. Geogr.*, *104*, 45–55.

Bennett, S. J., and J. L. Best (1995), Mean flow and turbulence structure over fixed, two-dimensional dunes: implications for sediment transport and bedform stability, *Sedimentology*, *42*, 491–513, doi:10.1111/j.1365-3091.1995.tb00386.x.

Best, J. (2005), The fluid dynamics of river dunes: A review and some future research directions, *J. Geophys. Res.*, *110*, F04S02, doi:10.1029/2004JF000218.

Best, J. L., and R. A. Kostaschuk (2002), An experimental study of turbulent flow over a low-angle dune, *J. Geophys. Res.*, *107*(C9), 3135, doi:10.1029/2000JC000294.

Best, J. L., S. J. Bennett, J. S. Bridge, and M. R. Leeder (1997), Turbulence modulation and particle velocities over flat sediment beds, *J. Hydraul. Eng.*, *123*, 1118–1129, doi:10.1061/(ASCE)0733-9429(1997)123:12(1118).

Brissette, M. B., J. E. Hughes-Clarke, and D. Cartwright (2001), Object detection using multibeam echo sounder temporal imagery, paper presented at the United States Hydrographic Conference, Hydrogr. Soc. of Am., Norfolk, Va.

Dinehart, R. L., and J. R. Burau (2005), Averaged indicators of secondary flow in repeated acoustic Doppler current profiler crossings of bends, *Water Resour. Res.*, *41*, W09405, doi:10.1029/2005WR004050.

Drake, T. G., R. L. Shreve, W. E. Dietrich, P. J. Whiting, and L. B. Leopold (1988), Bedload transport of fine gravel observed by motion-picture photography, *J. Fluid Mech.*, *192*, 193–217, doi:10.1017/S0022112088001831.

Fonseca, L., and L. Mayer (2007), Remote estimation of surficial seafloor properties through the application Angular Range Analysis to multibeam sonar data, *Mar. Geophys. Res.*, *28*, 199–126, doi:10.1007/s11001-007-9019-4.

Grass, A. J. (1970), Initial instability of fine bed sand, *Proc. Am. Soc. Civ. Eng.*, *96*, 619–632.

Grigoriadis, D. G. E., E. Balaras, and A. A. Dimas (2009), Large-eddy simulations of unidirectional water flow over dunes, *J. Geophys. Res.*, *114*, F02022, doi:10.1029/2008JF001014.

Gui, L. C., and W. Merzkirch (1996), A method of tracking ensembles of particle images, *Exp. Fluids*, *21*, 465–468, doi:10.1007/BF00189049.

Hughes-Clarke, J. E. (2006), Applications of multibeam water column imaging for hydrographic survey, *Hydrogr. J.*, *120*, 3–15.

Jackson, D. R., C. D. Jones, P. R. Rona, and K. G. Bermis (2003), A method for Doppler acoustic measurement of black smoker flow fields, *Geochem. Geophys. Geosyst.*, *4*(11), 1095, doi:10.1029/2003GC000509.

Kadota, A., and I. Nezu (1999), Three-dimensional structure of space-time correlation on coherent vortices generated behind dune crest, *J. Hydraul. Res.*, *37*, 59–80.

Kuhnle, R. A., and D. G. Wren (2009), Size of suspended sediment over dunes, *J. Geophys. Res.*, *114*, F02020, doi:10.1029/2008JF001200.

Lelouvetel, J., F. Bigillon, D. Doppler, I. Vinkovic, and J.-Y. Champagne (2009), Experimental investigation of ejections and sweeps involved in particle suspension, *Water Resour. Res.*, *45*, W02416, doi:10.1029/2007WR006520.

McLean, S. R., J. M. Nelson, and S. R. Wolfe (1994), Turbulence structure over two-dimensional bedforms: Implications for sediment transport, *J. Geophys. Res.*, *99*, 12,729–12,747, doi:10.1029/94JC00571.

McLean, S. R., J. M. Nelson, and R. L. Shreve (1996), Flow-sediment interactions in separating flows over bedforms, in *Coherent Flow Structures in Open Channels*, edited by P. J. Ashworth et al., pp. 203–226, John Wiley, Chichester, U. K.

Muste, M., K. Yu, I. Fujita, and R. Ettema (2009), Two-phase flow insights into open-channel flows with suspended particles of different densities, *Environ. Fluid Mech.*, *9*, 161–186, doi:10.1007/s10652-008-9102-7.

Nakayama, S., Y. Shimizu, M. W. Schmeeckle, and R. Akahori (2000), Numerical calculation of suspended sediments over sand waves, *Annu. J. Hydraul. Eng. Jpn. Soc. Civ. Eng.*, *44*, 629–634.

Nittrouer, J. A., M. A. Allison, and R. Campanella (2008), Bedform transport rates for the lowermost Mississippi River, *J. Geophys. Res.*, *113*, F03004, doi:10.1029/2007JF000795.

Parsons, D. R., J. L. Best, O. Orfeo, R. J. Hardy, R. Kostaschuk, and S. N. Lane (2005), Morphology and flow fields of three-dimensional dunes, Rio Paraná, Argentina: Results from simultaneous multibeam echo sounding and acoustic Doppler current profiling, *J. Geophys. Res.*, *110*, F04S03, doi:10.1029/2004JF000231.

Rennie, C. D., R. G. Millar, and M. A. Church (2002), Measurement of bedload velocity using an acoustic Doppler current profiler, *J. Hydraul. Eng.*, *128*, 473–483, doi:10.1061/(ASCE)0733-9429(2002)128:5(473).

Roy, A. G., T. Buffin-Bélanger, H. Lamarre, and A. D. Kirkbride (2004), Size, shape and dynamics of large-scale turbulent flow structures in a gravel-bed river, *J. Fluid Mech.*, *500*, 1–27, doi:10.1017/S0022112003006396.

Schmeeckle, M. W., and J. M. Nelson (2003), Direct numerical simulation of bedload transport using a local, dynamic boundary condition, *Sedimentology*, *50*, 279–301, doi:10.1046/j.1365-3091.2003.00555.x.

Simmons, S. M., et al. (2010), Monitoring suspended sediment dynamics using MBES, *J. Hydraul. Eng.*, *136*, 45–49, doi:10.1061/(ASCE)HY.1943-7900.0000110.

Stoesser, T., C. Braun, M. García-Villalba, and W. Rodi (2008), Turbulence structures in flow over two-dimensional dunes, *J. Hydrol. Eng.*, *134*(1), 42, doi:10.1061/(ASCE)0733-9429(2008)134:1(42).

Westerweel, J. (1997), Fundamental of digital particle image velocimetry, *Meas. Sci. Technol.*, *8*, 1379–1392, doi:10.1088/0957-0233/8/12/002.

J. Best, Departments of Geology and Geography and Ven Te Chow Hydrosystems Laboratory, University of Illinois at Urbana-Champaign, 1301 West Green St., Urbana, IL 61801, USA. (jimbest@illinois.edu)

J. Czuba, Watersheds and Ecology Section, U.S. Geological Survey, WA Water Science Center, 934 Broadway, Ste. 300, Tacoma, WA 98402, USA.

C. Malzone, Myriax Software Pty Ltd., 2877 Historic Decatur Rd., Ste. 400, San Diego, CA 92106, USA.

K. Oberg, Office of Surface Water, U.S. Geological Survey, 1201 W. University Ave., Ste. 100, Urbana, IL 61801, USA.

D. Parsons, School of Earth and Environment, University of Leeds, Woodhouse Lane, Leeds LS29JT, UK.

S. Simmons, Aquatec Group Ltd., High Street, Hartley Wintney RG27 8NY, UK.